Electronic Supplementary Material (ESI) for Journal of Materials Chemistry A.

Electronic Supplementary Information (ESI)

High-performance flexible and self-healable quasi-solid-state zinc-ion hybrid supercapacitor based on borax-crosslinked polyvinyl alcohol/nanocellulose hydrogel electrolyte

Minfeng Chen,[a] Jizhang Chen,*[a] Weijun Zhou,[a] Junling Xu[b] and Ching-Ping Wong*[bc]

[a] *College of Materials Science and Engineering, Nanjing Forestry University, Nanjing 210037, China*

[b] *Department of Electronic Engineering, The Chinese University of Hong Kong, NT, Hong Kong, China*

[c] *School of Materials Science and Engineering, Georgia Institute of Technology, Atlanta, United States*

E-mail addresses: jizhang.chen@hotmail.com (J. Chen) and cp.wong@mse.gatech.edu (C. Wong).

Experimental details

Preparation of cellulose fibers

Soybean stalks harvested from Jiangsu Province of China were washed with deionized (DI) water, cut into short pieces, and dispersed in an aqueous solution containing 2.5 M NaOH and 0.4 M Na_2SO_3. The dispersion was transferred into a Teflon-lined autoclave, which was then kept at 130 °C for 10 h. After hydrothermal treatment, the product was rinsed with boiling DI water for three times and then dispersed in 2.5 M H_2O_2 aqueous solution, which was subsequently kept at 110 °C for 4 h or 7 h. After washing with DI water for three times and then freeze drying, the product, namely cellulose fibers, can be obtained.

Mechanical measurements of hydrogel electrolytes

Tensile stress (σ)-strain (ε) tests were carried out on a UTM2502 universal testing machine (SANS Testing Machine Co. Ltd., Shenzhen, China) at a pulling rate of 30 mm min^{-1}. The samples were 30 mm× 15 mm× 0.5 mm in size. In order to evaluate the self-healing ability, the samples were halved by a knife, and then the two separate parts were put together for 20 s in air at room temperature without any external stimulus. After the self-healing process, the healed samples were tested under the same condition as original samples. All the mechanical testes were repeated five times. The self-healing efficiencies (η_σ and η_ε) are defined as:

$$\eta_\sigma = \frac{\sigma_{\text{healed}}}{\sigma_{\text{original}}} \times 100\% \qquad (1)$$

$$\eta_\varepsilon = \frac{\varepsilon_{\text{healed}}}{\varepsilon_{\text{original}}} \times 100\% \qquad (2)$$

where σ_{healed}, σ_{original}, $\varepsilon_{\text{healed}}$, and $\varepsilon_{\text{original}}$ represent tensile strength of original sample, tensile strength of healed sample, fracture elongation of original sample, and fracture elongation of healed sample, respectively. Compressive σ-ε measurements were also conducted on a UTM2502 universal testing machine at a crosshead speed of 15 mm min^{-1}. The samples were cylindrical in shape with 19 mm in diameter and 10 mm in height.

The dynamic strain sweep was performed on a MARS60 rheometer (Thermo Fisher Scientific Inc.) using a plate-and-plate geometry (diameter= 35 mm) with a gap of 100 μm at room temperature. The viscoelastic parameters (log mode), including shear storage modulus (G') and loss modulus (G'') with respect to the angular frequency (ω), were recorded at γ (strain) = 1% over the ω range of 0.1−100 Hz. The complex modulus (G*) and complex viscosity (η*) were calculated according to the following equations:

$$G^* = \sqrt{G'^2 + G''^2} \quad (3)$$

$$\eta^* = \frac{G^*}{\omega} \quad (4)$$

Ionic conductivity measurements of electrolytes

The ionic conductivity values of B-PVA/NFC and B-PVA hydrogel electrolytes were estimated by electrochemical impedance spectroscopy (EIS) measurements with an amplitude of 5 mV over a frequency from 100 kHz to 1 Hz. The EIS measurements were performed by sandwiching the hydrogel electrolytes between two stainless steel sheets. As for the liquid electrolyte, a Whatman GF/A filter paper filled with 2 M $ZnSO_4$ aqueous solution was used for EIS measurement under the same condition as hydrogel electrolytes. On the basis of the Nyquist plots, the ionic conductivity σ (mS cm^{-2}) could be calculated by the following equation:

$$\sigma = \frac{100d}{RA} \quad (5)$$

where R (Ω) is the intercept with real axis, and d (mm) and A (cm^2) represent the thickness and area of hydrogel electrolytes or separator, respectively.

Water content measurements of hydrogels

The hydrogel samples (W_h weight) were dried at 50 ºC under vacuum until a steady weight (W_d) was reached. The water content W was calculated as:

$$W = \frac{W_\mathrm{h} - W_\mathrm{d}}{W_\mathrm{h}} \times 100\% \qquad (6)$$

Peeling measurements of hydrogels

The peeling measurements were conducted using a MK-BL-X90 peeling analyzer (MAIKE Instrument Equipment Co. Ltd., Dongguan, China). A zinc foil was laid flat on a B-PVA/NFC hydrogel. The tests were performed with a standard 90° peeling angle at a constant peeling speed of 20 mm min^{-1}.

Fabrication of the AC-paper

In a typical preparation of the AC-paper, 41.9 mg cellulose fibers (4 h for H_2O_2 treatment), 41.9 mg carbon black (from Alfa Aesar), 41.9 mg AC (from XFNANO), and 15 mg cetyltrimethyl ammonium bromide (CTAB) were dispersed in 30 mL DI water with the assistance of ultrasonication, and then vacuum filtered through a filter membrane (4 mm diameter, 0.22 μm pore size). After washing with DI water for three times, the obtained AC-paper can be easily peeled off from the filter membrane, then dried at 80 °C in an oven overnight, and finally pressed at 10 MPa for 1 min.

Supplementary figures

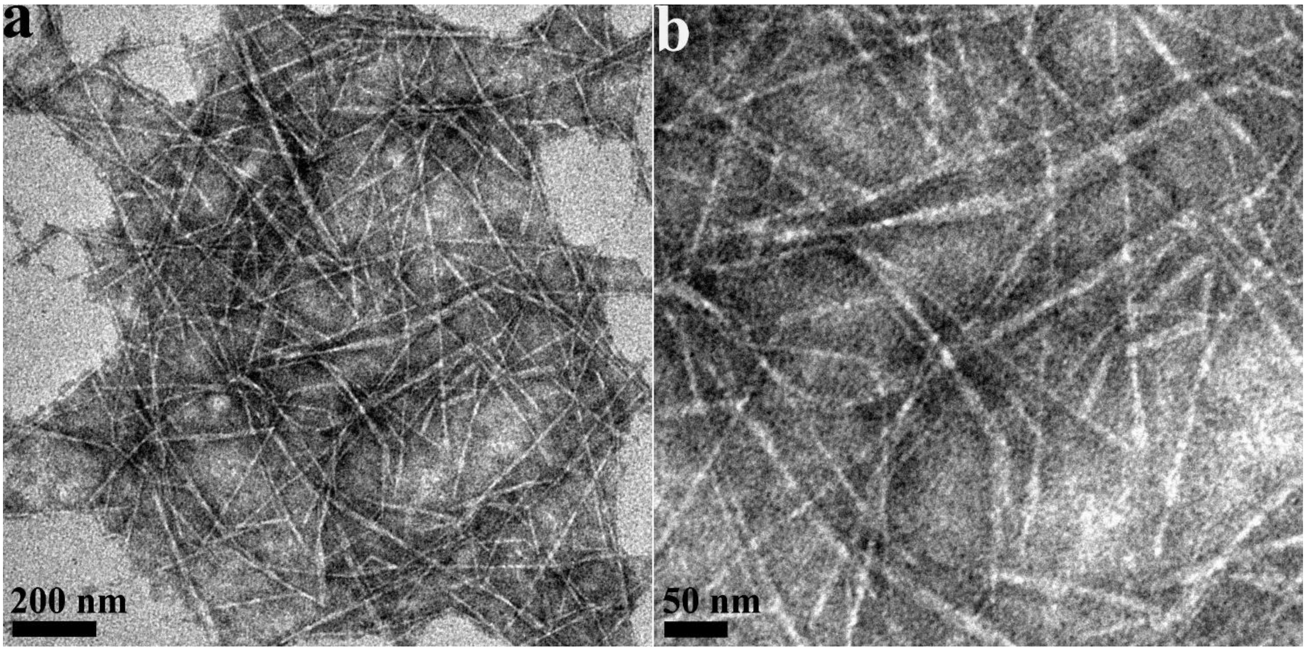

Fig. S1 (a,b) TEM images of NFC. The NFC was negatively stained with phosphotungstic acid to enhance the contrast.

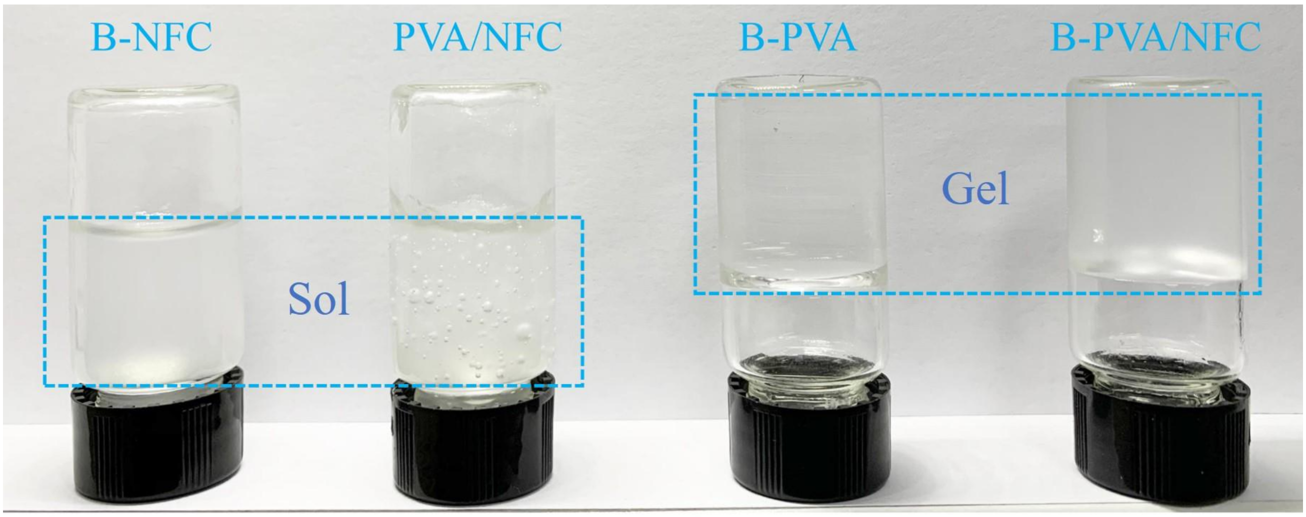

Fig. S2 Photographs of B-NFC, PVA/NFC, B-PVA, and B-PVA/NFC.

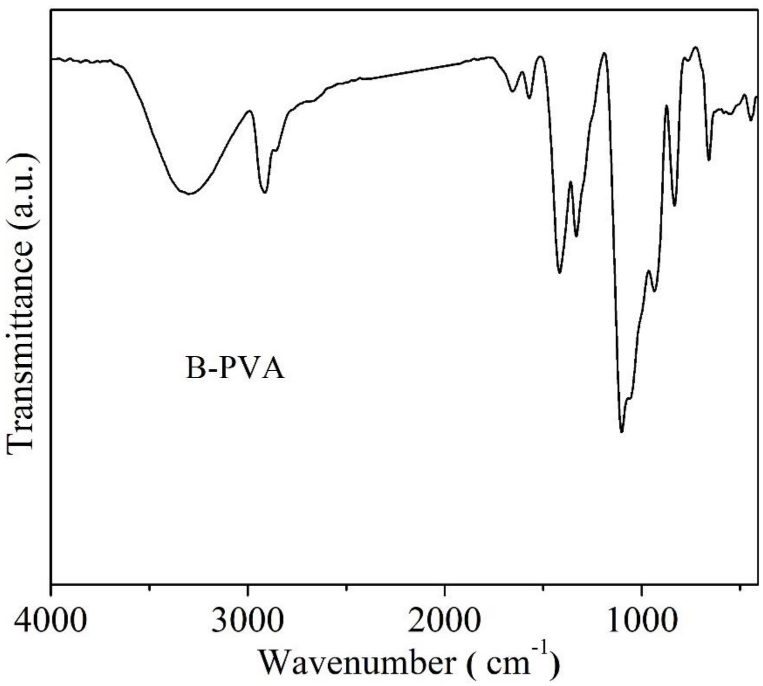

Fig. S3 FTIR spectrum of the freeze-dried B-PVA.

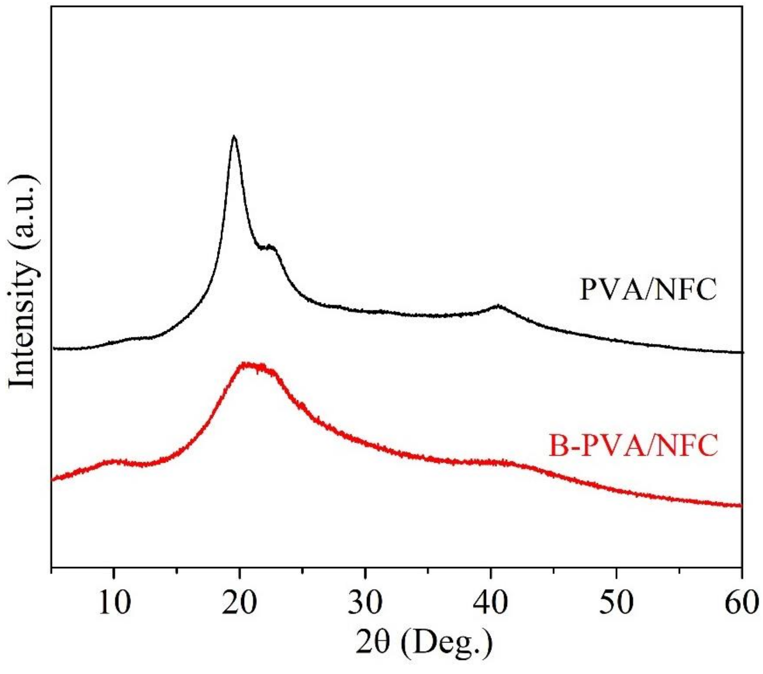

Fig. S4 XRD pattern of the freeze-dried PVA/NFC, in comparison with that of B-PVA/NFC.

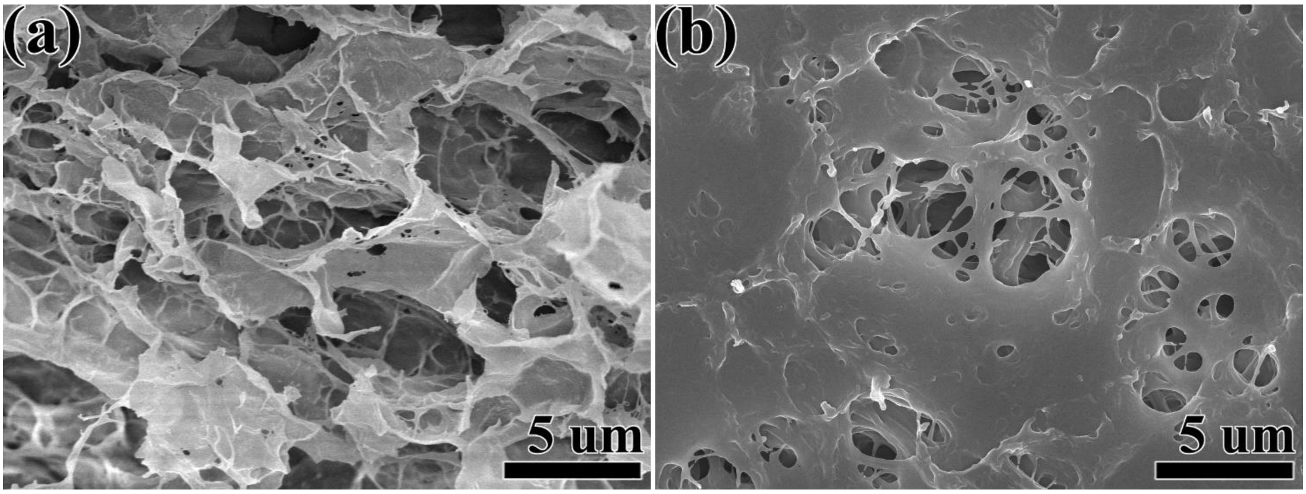

Fig. S5 SEM images of the freeze-dried (a) B-PVA/NFC and (b) B-PVA.

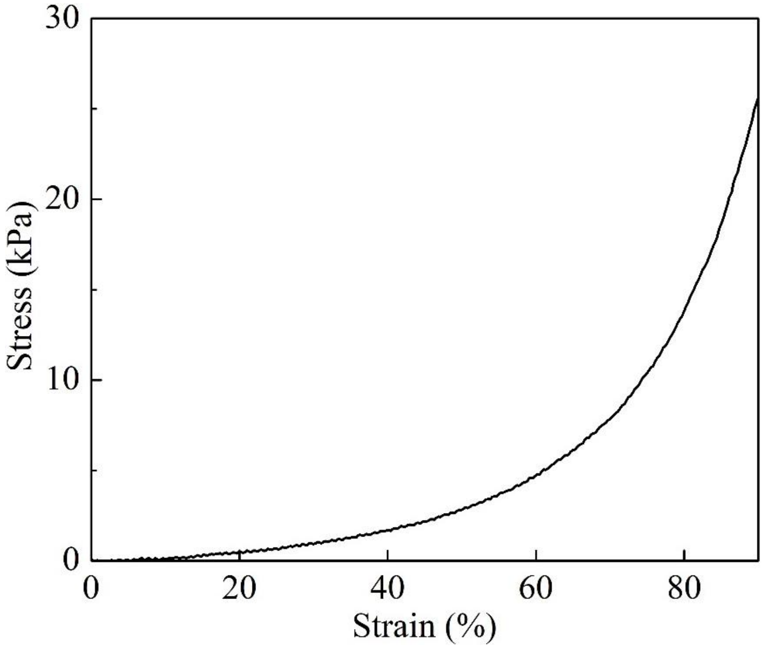

Fig. S6 Compressive *σ*-*ε* curve of the B-PVA/NFC hydrogel electrolyte.

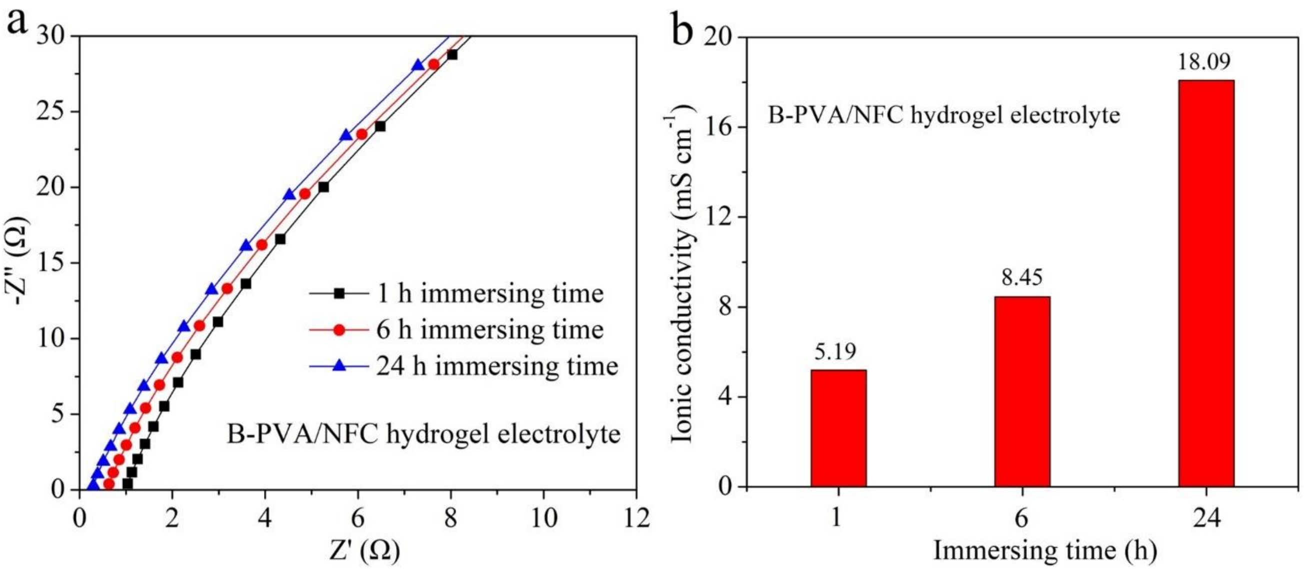

Fig. S7 (a) Nyquist plots and (b) ionic conductivity values of the B-PVA/NFC hydrogel electrolyte after immersing in 2 M $ZnSO_4$ aqueous solution for different time.

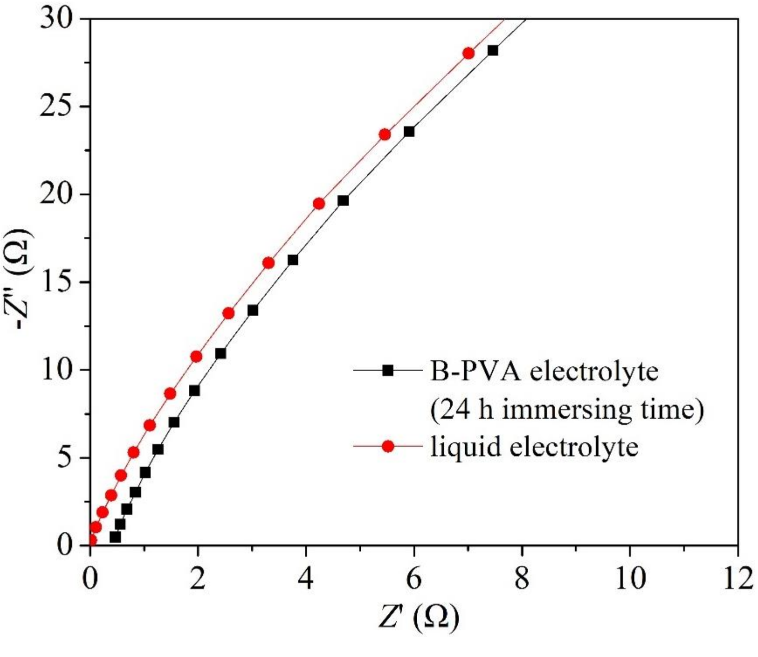

Fig. S8 Nyquist plots of the B-PVA and liquid electrolytes.

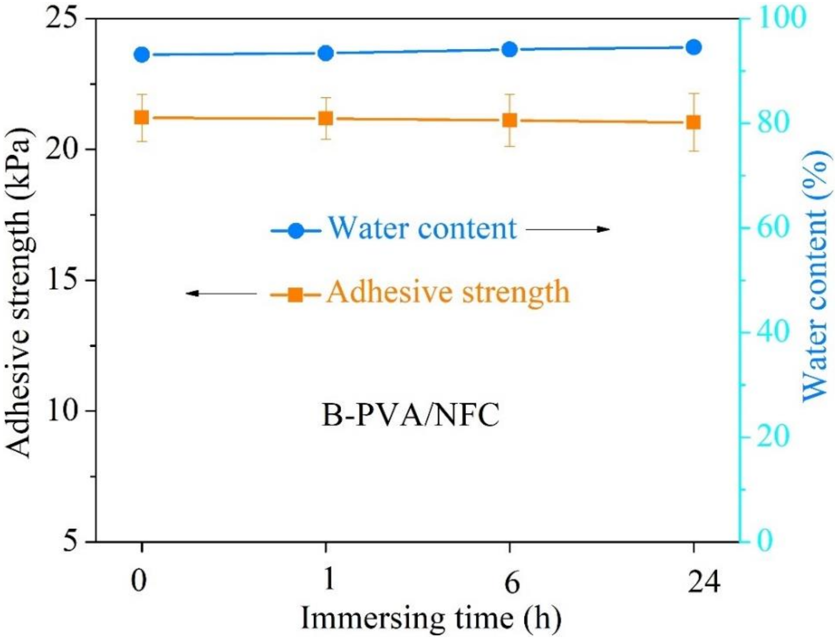

Fig. S9 Adhesive strength and water content of the B-PVA/NFC after immersing in 2 M $ZnSO_4$ aqueous solution for different time (0 h represents the as-prepared B-PVA/NFC hydrogel before immersing).

Fig. S10 Photographs of peeling tests.

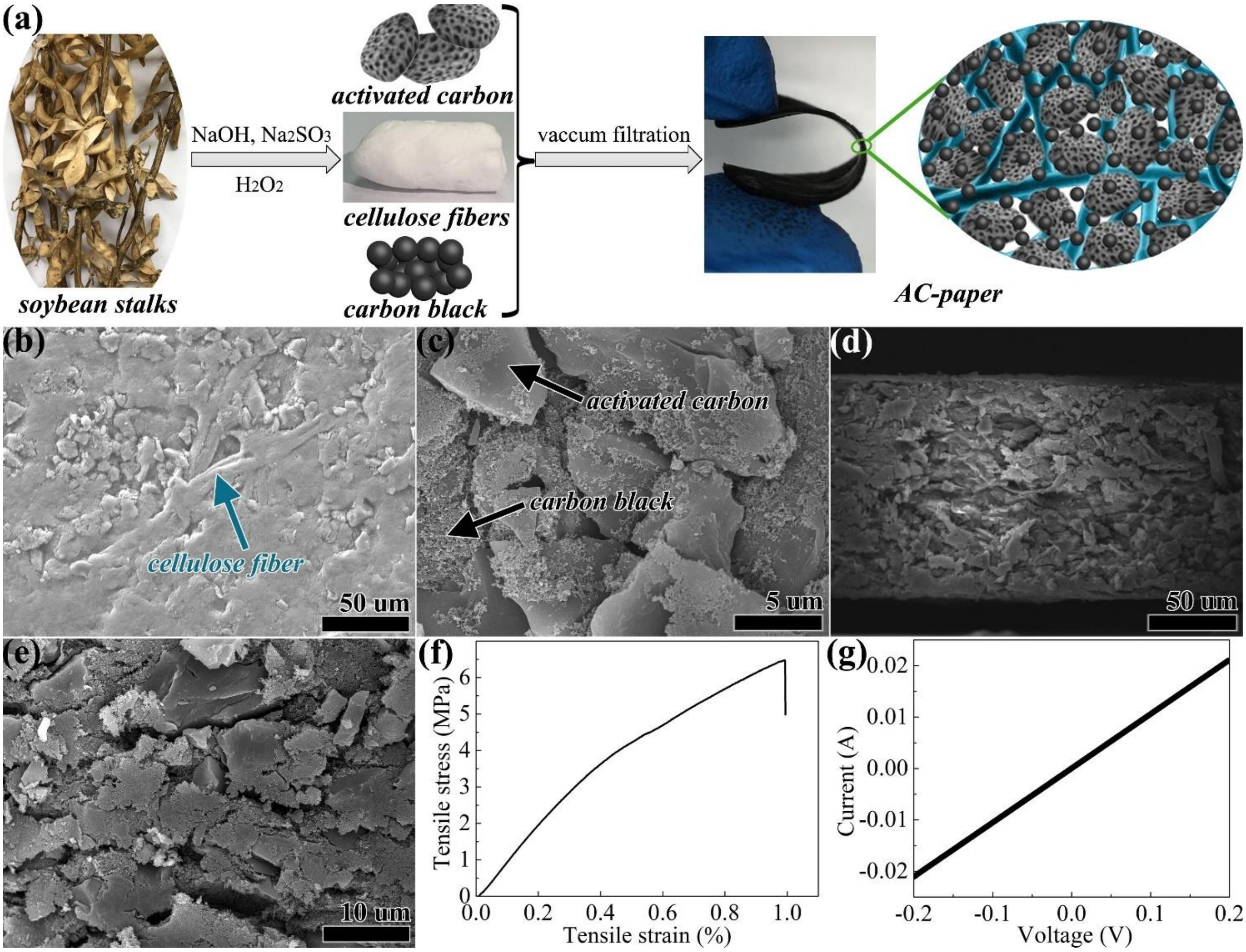

Fig. S11 (a) Schematic illustration of the preparation process and photographic image, (b,c) surface SEM images, (d,e) cross-sectional SEM images, (f) tensile strain-stress curve, and (g) *I-V* curve of the AC-paper.

Fig. S11a schematically illustrates the fabrication procedure of AC-paper. Cellulose fibers were refined from soybean stalks *via* a two-step process. In the first step, the soybean stalks were hydrothermally treated in a mixed aqueous solution containing NaOH and Na_2SO_3. As is well known, crop straws are comprised by cellulose, hemicellulose, and lignin. During the hydrothermal treatment, lignin and hemicellulose were substantially removed from soybean stalks by the sulfite-containing alkaline solution, while most of cellulose was preserved, due to the different stability and reactivity of these three components.[1,2] In the second step, lignin and hemicellulose were further removed by H_2O_2, which is a bleaching agent in the paper making industry. Then, the obtained cellulose fibers were mixed with AC and carbon black with a mass ratio of 1: 1: 1 to form an aqueous suspension. A small amount of CTAB was also added, in order to help AC and carbon black disperse in the suspension. The suspension was subsequently filtered under vacuum assistance, producing AC-paper, which is free-standing, flexible, and bendable, as shown in Fig. S11a. From surface and cross-sectional SEM images in Fig. S11b‒e, it can be seen that cellulose fibers, AC, and carbon black are homogeneously mixed and organize in a dense and compact fashion. Fig. S11f shows the tensile strain-stress curve of AC-paper. It manifests a high strength of 6.46 MPa and fracture elongation around 1%. The electrical conductivity of AC-paper was estimated by a typical *I-V* method using CHI660E electrochemical workstation. According to the *I-V* curve in Fig. S11g, the electrical conductivity of AC-paper is 1.2×10^3 S m^{-1}.

Fig. S12 The photograph of measuring the thickness of AC-paper with a micrometer caliper.

The thickness of AC-paper is measured to be 141± 10 μm with a micrometer caliper (see Fig. S12). And the average mass loading of AC in the paper electrode is determined to be ~4 mg cm^{-2}.

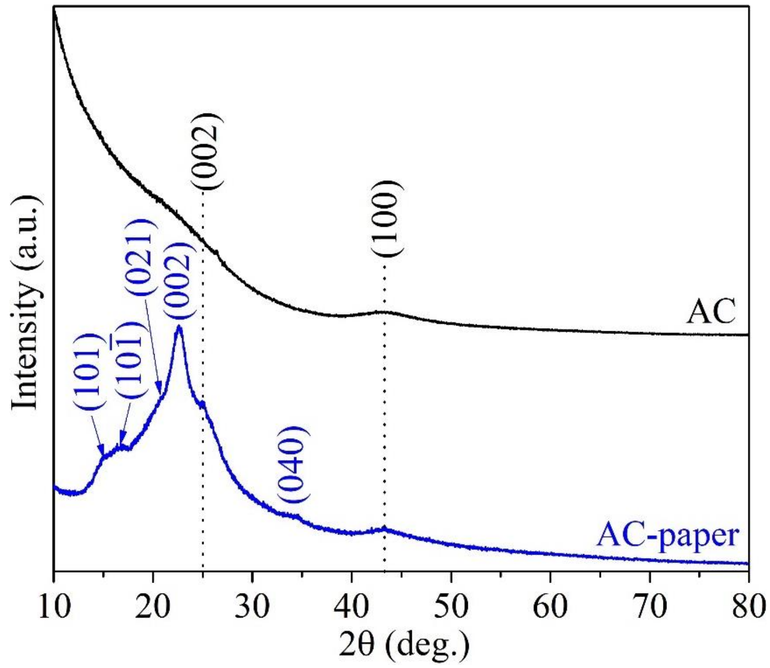

Fig. S13 XRD patterns of AC and AC-paper.

The broad humps of AC come from (002) and (100) planes of pseudographitic domains.[3] Except for these two humps, all the peaks of AC-paper can be indexed as the crystalline planes of cellulose I.[4,5] Compared to standard cellulose I, the corresponding peaks in AC-paper is much broader, due to the alkalization and bleaching treatments, which destroy the crystalline structure of cellulose and reduce the density of hydrogen bonds. Besides, there exists a small amount of lignin in the AC-paper, which cannot be detected by XRD characterization due to its low crystallinity, but is beneficial to the mechanical robustness of the paper electrode.[6,7]

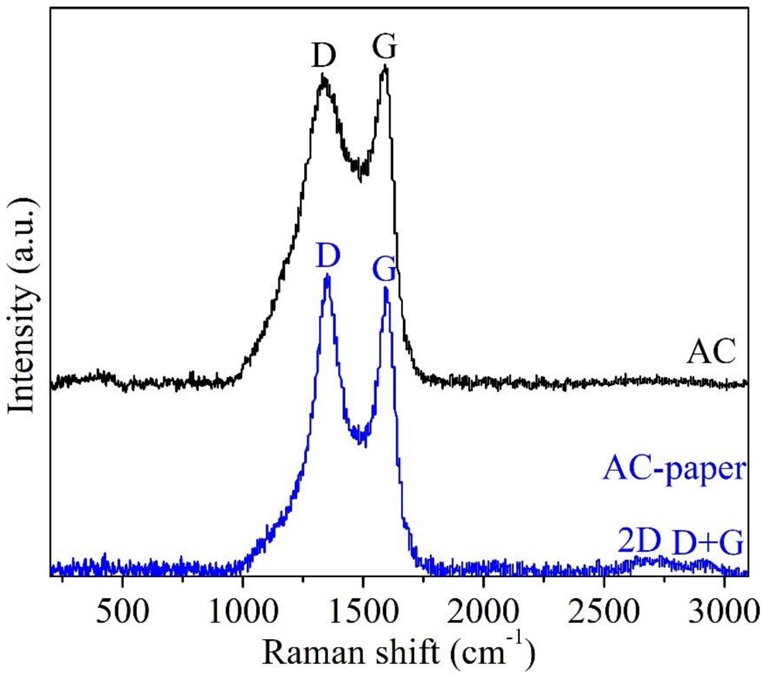

Fig. S14 Raman spectra of AC and AC-paper.

The Raman spectrum of AC exhibits typical characteristic of carbonaceous materials, that is, D band at ~1340 cm^{-1} arising from disorder in sp^2-hybridized carbon and G band at ~1590 cm^{-1} originating from in-plane C-C stretching, along with weak 2D and D+G bands.[3] Compared with AC, the AC-paper shows a higher value of I_D/I_G, resulting from lower graphitic degree of carbon black than that of AC.[6] Besides, the absence of cellulose in the Raman spectrum of AC-paper is due to that the Raman response from cellulose is much lower than that of carbonaceous materials.[6]

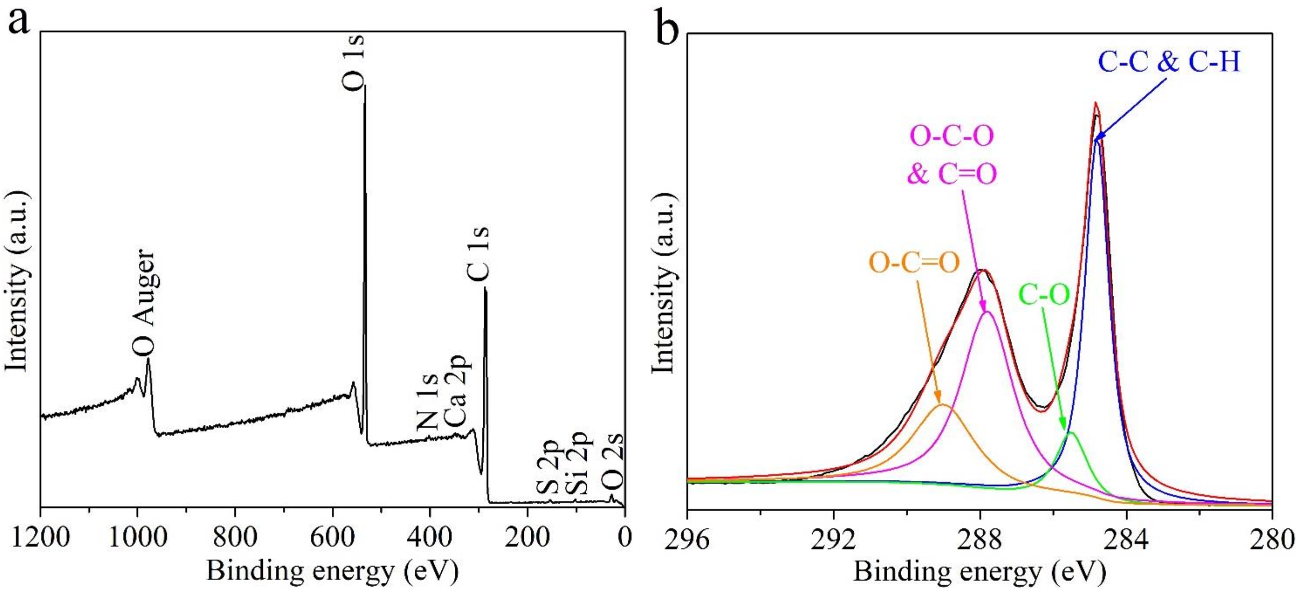

Fig. S15 (a) Survey and (b) high-resolution C 1s XPS spectra of AC-paper

XPS measurement was conducted to study the surface chemistry of AC-paper. The survey spectrum indicates the AC-paper mainly consists of C and O elements (H is undetectable by XPS). In addition to C and O, trace amounts of Si, S, Ca and N exist in the AC-paper, which are probably the residual of some substances in soybean stalks.[8] The high-resolution C 1s spectrum of AC-paper can be deconvoluted into four sub-peaks at 284.8, 285.5, 287.8, and 289.0 eV, corresponding to C–C (& C–H), C–O, O–C–O (& C=O), and O–C=O bondings, respectively.[7]

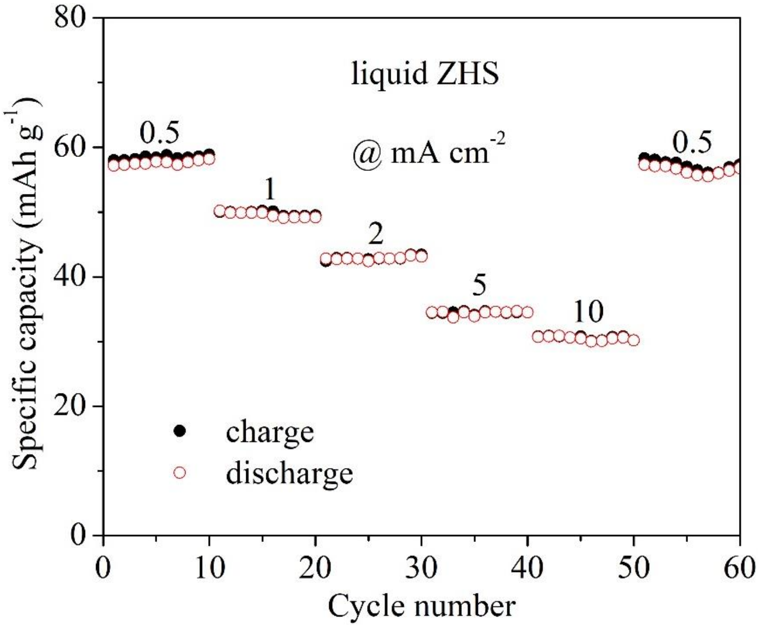

Fig. S16 Rate performance of the liquid ZHS.

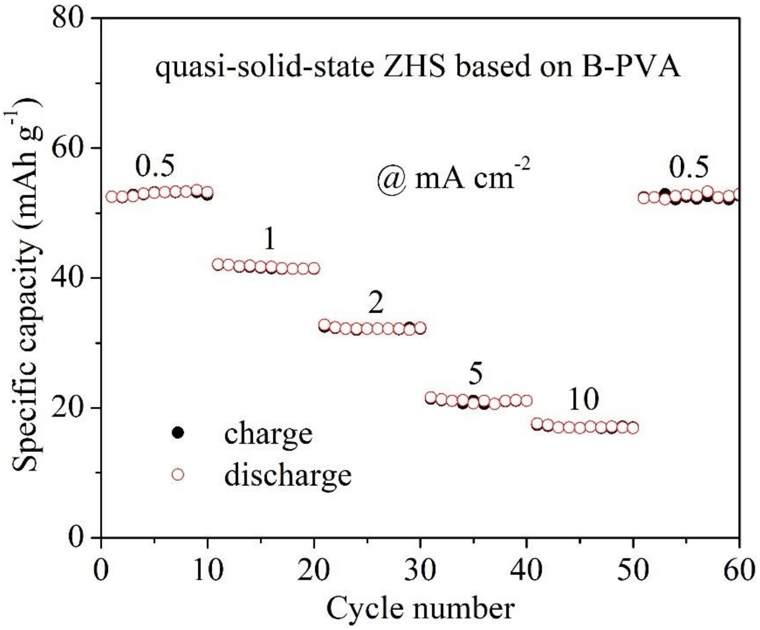

Fig. S17 Rate performance of the quasi-solid-state ZHS device based on B-PVA hydrogel electrolyte.

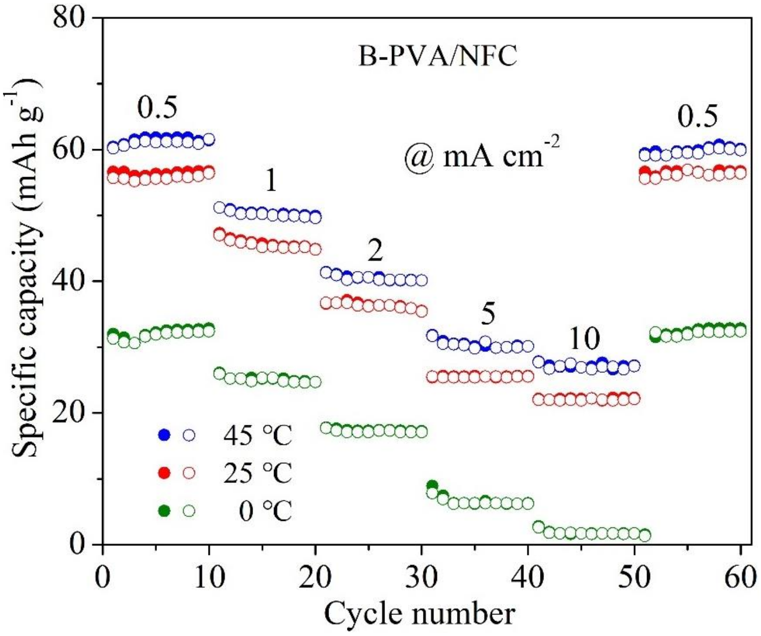

Fig. S18 Rate performances of the quasi-solid-state ZHS device based on B-PVA/NFC hydrogel electrolyte at different temperature.

Supplementary videos

Video S1 Demonstration of a B-PVA/NFC ZHS device under repeated bending to power an electric fan.

Video S2 Demonstration of a B-PVA/NFC ZHS device under repeated bending to power a timer.

References

1 J. W. Song, C. J. Chen, S. Z. Zhu, M. W. Zhu, J. Q. Dai, U. Ray, Y. J. Li, Y. D. Kuang, Y. F. Li, N. Quispe, Y. G. Yao, A. Gong, U. H. Leiste, H. A. Bruck, J. Y. Zhu, A. Vellore, H. Li, M. L. Minus, Z. Jia, A. Martini, T. Li and L. B. Hu, *Nature*, 2018, **554**, 224.

2 C. J. Chen, J. W. Song, S. Z. Zhu, Y. J. Li, Y. D. Kuang, J. Y. Wan, D. Kirsch, L. S. Xu, Y. B. Wang, T. T. Gao, Y. L. Wang, H. Huang, W. T. Gan, A. Gong, T. Li, J. Xie and L. B. Hu, *Chem*, 2018, **4**, 544-554.

3 J. Ding, H. L. Wang, Z. Li, K. Cui, D. Karpuzov, X. H. Tan, A. Kohandehghan and D. Mitlin, *Energy Environ. Sci.*, 2015, **8**, 941-955.

4 S. Park, J. O. Baker, M. E. Himmel, P. A. Parilla and D. K. Johnson, *Biotechnol. Biofuels*, 2010, **3**, 10.

5 L. K. Xiong, G. M. Yu and C. Y. Yin, *Fiber. Polym.*, 2017, **18**, 88-94.

6 J. Chen, K. Fang, Q. Chen, J. Xu and C.-P. Wong, *Nano Energy*, 2018, **53**, 337-344.

7 T. G. Yun, D. Kim, S.-M. Kim, I.-D. Kim, S. Hyun and S. M. Han, *Adv. Energy Mater.*, 2018, **8**, 1800064.

8 J. Z. Chen, X. Y. Zhou, C. T. Mei, J. L. Xu, S. Zhou and C. P. Wong, *J. Power Sources*, 2017, **342**, 48-55.